

PHANGS-MUSE

I. Overview of Data Release 1

Eric Emsellem^{1,2}, Francesco Belfiore¹, Ismael Pessa³ and et al. (authors in no particular order)

¹ European Southern Observatory, Karl-Schwarzschild-Str. 2, Garching bei München, 85748, Germany

² Univ Lyon, Univ Lyon1, ENS de Lyon, CNRS, Centre de Recherche Astrophysique de Lyon UMR5574, F-69230 Saint-Genis-Laval France

³ Max Planck Institut für Astronomie, Königstuhl 17, 69117 Heidelberg, Germany

Received XXX, 2019; accepted

ABSTRACT

Most updated version to be found on <https://www.overleaf.com/project/5cf919e60be68b38b40832ef>. Summary of methods for the PHANGS-MUSE reduction and analysis code. Summary of data release 1

1. Introduction

2. The data reduction pipeline

2.1. Pipeline softwares

We are using the latest version of the MUSE pipeline, version 2.6.2-1 (Weilbacher et al.).

We are using a wrapper (pymusepipe), written in python (emsellem/pymusepipe), to automatically process data from a single pointing. The package also includes a module for alignment and combining of pointings.

2.2. Processing steps

Steps are: deriving the master bias and flat, computing the wavelength calibration solution, the lsf, dealing with the twilight. Calibration files (twilights, flats etc) are selected according to their time of observations.

With such calibration frames, we proceed with each individual exposures and apply a standard star correction for absolute flux. We then derive a sky spectrum, prepare the alignment images from the target exposures, find approximate offsets and combine them into a single cube.

Alignment: we use a dedicated alignment module in pymusepipe starting from the MUSE derived offsets and using reconstructed images with a specific WFI broad band filter. This is done semi-manually by using contours and residuals w.r.t. a reference WFI image. During that step we also calculate the flux scaling which is then saved into the OFFSET table to be used during the combine step.

3. The data analysis pipeline

The analysis pipeline for the PHANGS-MUSE data is largely derived from the GIST code (?) by Adrian Bittner. The code is available on GitLab.¹ The main changes with respect to the public version of the GIST code include the use of ppXF(??) instead

¹ <https://gitlab.com/francbelf/ifu-pipeline>, private repository, will become public with data release

of GANDALF (?) for the emission lines analysis and a different philosophy for the stellar population module (developed for PHANGS by Ismael Pessa). The pipeline is modular, and it saves intermediate data products after each stage, allowing the user to re-run specific stages without having to start from scratch. Note that 2D maps of all quantities are only produced at the end, but the user can force the creation of the maps if the pipeline failed in some cases. The pipeline can be parallelised in its fitting stages, although non-fitting stages are still limited to using a single core. Below we give some details regarding the pipeline and the parameters used for the team data release 1 (DR1).

3.1. Binning

The continuum S/N is computed in a user-provided wavelength range (default is 5300-5500 Å). The stellar kinematics is computed on a set of Voronoi bins (?) with a target S/N of 30. The stellar population analysis is carried out on the same bins (although there are plans to further develop the code to remove this limitation).

The emission lines can be fitted on three different binning schemes.

- on the same Voronoi bins as the stellar kinematics
- on single spaxels
- on a set of Voronoi bins based on the H α amplitude over noise. In order to calculate the H α amplitude over noise a simple integration of the flux around the position of the H α line is performed on the continuum subtracted spectra (using the best-fit continuum from the stellar kinematics stage).

3.2. Stellar kinematics

The stellar kinematics are derived with a subset of the eMILES stellar population models using a Chabrier IMF, Basti isochrones, base α/Fe . We only consider ages > 0.15 Gyr in order to have the full wavelength coverage out to 9000 Å (spectral coverage redder than 8950 Å is only available for > 0.15 Gyr). However right now we are only fitting out to 7000 Å to make your life simpler. The spectral resolution of the eMILES

is similar (or lower) to that of the MUSE data at the red end of the spectrum.² The templates are convolved to the spectral resolution of the data. If in some wavelength range the templates have lower resolution than the data no convolution is performed. At this stage the errors on the kinematic parameters are formal errors. Code is in place to perform an MCMC-based error estimate but will not be done in the first team release. During this fitting stage pPXF fits up to the 4th order in the stellar kinematics LOSVD (v , σ , h_3 and h_4). We also make use of additive polynomials (12 order) and no multiplicative polynomials.

3.3. Emission lines

Emission lines are fitted by making a new call to pPXF, where the emission lines are treated as additional Gaussian templates, and the stellar continuum is fitted simultaneously. The stellar kinematics is fixed to that of the previous stage in case the emission lines are fitted in single spaxels or in the same Voronoi bins as the emission lines. In the case where the emission lines are fitted on a different set of Voronoi bins the treatment of stellar kinematics is still tbd (but this mode is not use in DR1 anyway). The kinematic parameters of the emission lines (v and σ) are tied in three groups

1. Balmer lines: $H\alpha$, $H\beta$.
2. Low-ionization lines: [OI] $\lambda\lambda 6300, 64$, [NI] $\lambda\lambda 5197, 5200$, [NII] $\lambda\lambda 6548, 84$, [SII] $\lambda\lambda 6717, 31$, [SII] $\lambda\lambda 4068, 76$, [NII] $\lambda 5754$, [OII] $\lambda\lambda 7319, 30$.
3. High-ionization lines: HeI $\lambda 5875$, HeII $\lambda 4687$, [OIII] $\lambda\lambda 4959, 5007$, [SIII] $\lambda\lambda 9068, 9530$.

It has demonstrated that not tying the velocity and dispersion of the $H\beta$ to that of $H\alpha$ leads to a large fraction of spaxels/bins having unphysical Balmer decrements (see discussion on Slack). During the emission lines fit pPXF is run with no additive and 8th order multiplicative polynomials.

3.4. Stellar populations

The stellar population module employs pPXF with fixed stellar kinematics and masks the regions around all emission lines. Regions of the spectrum particularly affected by sky lines are also masked. The fit is performed in two stages. In the first stage the stellar extinction is determined, while in the second iteration the stellar extinction is fixed and multiplicative polynomials of 12th order are used to correct for residual inaccuracies in the relative flux calibration. This two-tiered procedure was demonstrated to be necessary to overcome ‘wobble-like’ differences in the spectra of regions in common between two MUSE pointings (see work by Ismael). We have opted against the use of regularisation, as defined in ?. Instead we perform a set of MCMC simulations to estimate the uncertainty in the recovered stellar population parameters. At the moment non MCMC step is employed in the first stage, where extinction is determined, and therefore no error is available on the stellar $E(B-V)$. Stellar mass surface densities and mass-weighted age and metallicities are calculated automatically by the pipeline by taking into account the M/L ratio of the stellar SSP templates. Other quantities related to the SFH can be computed following the instructions here (make Jupyter notebooks). As a reminder, a Chabrier IMF is assumed.

² <http://www.iac.es/proyecto/miles/pages/spectral-energy-distributions-seds/e-miles.php>

3.5. Output files

The pipeline produced intermediate output files after each fitting stage. However most users will only be interested in the final set of 2D maps, which included all main quantities computed by the various fitting stages. These maps are consolidated in the so-called MAPS files and its content is given in Table 1.

3.5.1. The MAPS file

See Table 1.

MUST READ!

1. Velocities are computed with respect to a systemic velocity taken from the z0mgs database³)
2. There is a difference in the way the velocity dispersions for gas and stars are reported. The stellar velocity dispersion is reported as the astrophysical dispersion, while the velocity dispersion of the lines is reported as the observed velocity dispersion. To obtain the astrophysical velocity dispersion for the emission lines the relevant SIGMA_CORR extension contains the instrumental sigma at the wavelength of the emission line and ought to be subtracted in quadrature.
3. No error is reported for the stellar $E(B-V)$. This quantity is the one which is likely to suffer from the largest pointing-to-pointing variations, which remain unexplained (work in progress). We strongly caution against the indiscriminate use of these maps for science.

3.5.2. Reference files

We refer to all other files produced by the pipeline are reference output files. These files are useful as a starting point of a future run of the pipeline if one particular stage has already been performed (for example, in order to skip the Voronoi binning stage, the user can simply copy the relevant reference files from a previous run of the pipeline into the output folder of the new pipeline run). The reference files also contain extra information which is not propagated to the MAPS files, including all best-fit models for the different stages of the pipeline and the full output of the MCMC runs for the stellar population stage, which can be useful to compute other quantities related to the SFH (see Jupyter notebook). Moreover, by providing a user-supplied binning map the pipeline can be used to fit, for example, a sample of Hii regions defined as a set of masks (see Jupyter notebook).

4. Point Spread Function

Convolution method: describe

5. Spectral Resolution

LSF method: describe

6. Summary of DR1

7. Conclusions

Acknowledgements.

References

³ <https://github.com/akleroy/z0mgs>

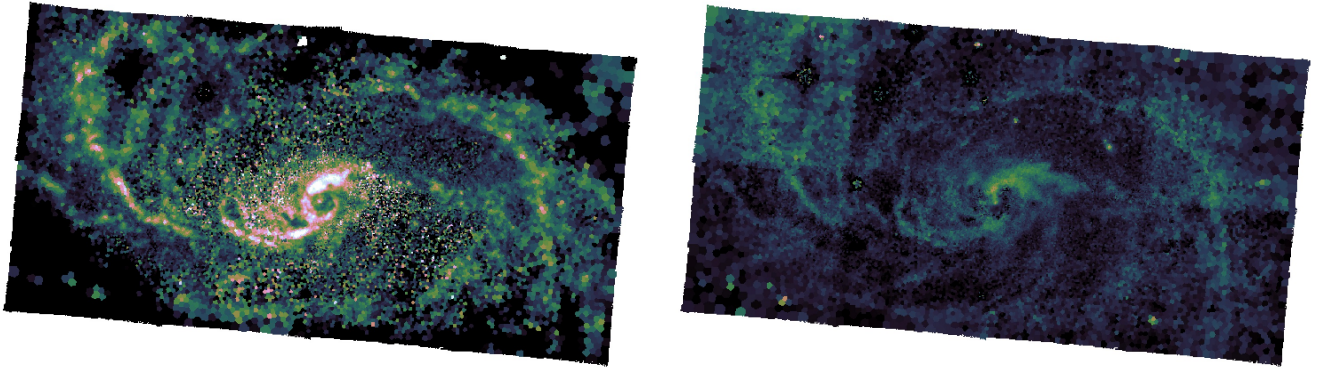


Fig. 1. Left: Gas E(B-V) computed from the Balmer Decrement based on the MAPS file and binned on the same binning scheme as the stellar populations. The colour-bar goes from 0-1 mag. Right: E(B-V) of the stars, on the same colour-bar. One can see that the stellar E(B-V) is tracing similar structures, although a jump is evident in the top-left MUSE pointing, which shows an artificially higher median level of extinction. Credit: Brent Groves.

Table 1. MAPS file produced by the PHANGS DAP

| Extension name | Description |
|--|---|
| Binning | |
| ID | unique ID for each spaxel |
| FLUX | white-light image computed in the wavelength range used for S/N computation |
| SNR | continuum S/N ratio for individual spaxels |
| SNRBIN | continuum S/N for each Voronoi bin |
| BIN_ID | unique ID for each Voronoi bin, unbinned spectra have negative bin IDs |
| Stellar kinematics | |
| V_STARS | stellar velocity [km/s], after subtracting the systemic velocity |
| FORM_ERR_V_STARS | formal velocity error |
| ERR_V_STARS | MCMC-calculated error for velocity (if available) |
| SIGMA_STARS | stellar velocity dispersion [km/s] |
| FORM_ERR_V_STARS | formal sigma error |
| ERR_SIGMA_STARS | MCMC-calculated error for sigma (if available) |
| eg. H3_STARS | higher order moments of the stellar LOSVD (if available) |
| eg. FORM_ERR_H3_STARS | formal errors in the high-order moments |
| eg. ERR_H3_STARS | MCMC errors for higher order moments |
| Stellar populations (be aware of limitations described in sec. 3.5.1) | |
| STELLAR_MASS_DENSITY | stellar mass surface density [M_{\odot}/pc^2] |
| STELLAR_MASS_DENSITY_ERR | error in the above |
| AGE_MW | $\log(\text{Age}/\text{yr})$, where the Age is mass weighted |
| AGE_MW_ERR | error in the above |
| Z_MW | [Z/H] mass-weighted |
| Z_MW_ERR | error in the above |
| AGE_LW | $\log(\text{Age}/\text{yr})$, where the Age is luminosity weighted |
| AGE_LW_ERR | error in the above |
| Z_LW | [Z/H] luminosity-weighted |
| Z_LW_ERR | error in the above |
| EBV_STARS | E(B-V) of the stellar component [mag] |
| Emission lines | |
| *emline = emission line string id listed in Table 2 | |
| BIN_ID_LINES | unique bin for emission lines |
| emline_FLUX | emission line flux [$10^{-20} \text{erg/s/cm}^2/\text{spaxel}$] |
| emline_FLUX_ERR | emission line flux error |
| emline_VEL | emission line velocity [km/s] |
| emline_VEL_ERR | emission line velocity error |
| emline_SIGMA | emission line velocity dispersion [km/s] |
| emline_SIGMA_ERR | emission line velocity dispersion error |
| emline_SIGMA_CORR | instrumental velocity dispersion at the position of the line |

Table 2. Wavelengths and ionization potential of the relevant ion for each emission line fit in DR1. Ritz wavelengths in vacuum are taken from the National Institute of Standards and Technology (NIST; <http://physics.nist.gov/PhysRefData/ASD/Html/help.html>). The DAP string name is used to identify the correct extinction in the MAPS files. Ionization potentials are taken from ?. Lines redder than $\sim 7000 \text{ \AA}$ are currently not fitted in DR1.

| line name | wavelength (vacuum) [\AA] | DAP string name | Ionization potential [eV] | Fixed ratio |
|-----------------------|--------------------------------------|-----------------|---------------------------|-----------------------------|
| Hydrogen Balmer lines | | | | |
| H β | 4862.691 | HB4861 | 13.60 | no |
| H α | 6564.632 | HA6562 | 13.60 | no |
| Low ionization lines | | | | |
| [NI] λ 5197 | ?? | NI5197 | 0.0 | no |
| [NI] λ 5200 | ?? | NI5200 | 0.0 | no |
| [OI] λ 6300 | 6302.04 | OI6300 | 0.0 | no |
| [OI] λ 6364 | 6365.535 | OI6363 | 0.0 | 0.328 [OI] λ 6300 |
| [NII] λ 6548 | 6549.86 | NII6548 | 14.53 | 0.327 [NII] λ 6584 |
| [NII] λ 6584 | 6585.271 | NII6583 | 14.53 | no |
| [SII] λ 6717 | 6718.294 | SII6716 | 10.36 | no |
| [SII] λ 6731 | 6732.674 | SII6730 | 10.36 | no |
| [NII] λ 5754 | ?? | NII5754 | 14.53 | no |
| High ionization lines | | | | |
| [OIII] λ 4959 | 4960.295 | OIII4958 | 35.12 | 0.340 [OIII] λ 5007 |
| [OIII] λ 5007 | 5008.240 | OIII5006 | 35.12 | no |
| HeI λ 5876 | 5877.243 | HeI5877 | 24.58 | no |